SUPPLEMENTAL MATERIALS

SUPPLEMENTAL METHODS

Bone marrow harvest and flow cytometry

Bone marrow (BM) was harvested, processed, and stained in cold PBS with 2% heat-inactivated FBS. Red blood cells were lysed in ACK Lysing Buffer (Gibco) for 2 min on ice. Cells were stained in the presence of Fc Block (BD Biosciences Cat# 553142, RRID:AB_394657) with the exception of the hematopoietic progenitor panel utilized in Figure 7. Doublets were excluded in all analyses and sorts. LIVE/DEAD Aqua (Invitrogen), Zombie Violet (BioLegend), or DAPI (Sigma) were used as viability stains to exclude dead cells from analyses and sorts.

Processing of lungs and bronchoalveolar lavage

24 hours post-inhalation mice were humanely euthanized for collection of whole lung for histology or bronchoalveolar lavage (BAL) as described previously.[1,2] Briefly, perfused and fixed mouse lungs were imbedded in paraffin, sectioned, and stained with hematoxylin and eosin. Cytospins of BAL fluid were stained with Hema 3 Stat Pack (Fisher Scientific) and differential was determined by manual counting an entire field of view. All light microscopy images were acquired using an Olympus BX41 microscope. Total white blood cell (WBC) count per mL of BAL fluid was determined by performing red blood cell lysis of the BAL fluid followed by a manual count of the remaining WBCs using a hemacytometer. Absolute neutrophil counts per mL of BAL fluid were determined by multiplying the WBC counts by the percent neutrophil differential determined by cytospin. Total protein was determined using a Bradford Assay (Bio-Rad) and a bovine serum albumin standard curve. Multiplex quantification of inflammatory factors in the BAL was performed using the CBA flex sets (BD) as described.

Western blots

For all Western blots, equivalent numbers of cells were stimulated, washed, and lysed in RIPA buffer supplemented with protease inhibitors (Sigma-Aldrich). Samples were boiled in LDS Sample Buffer with Sample Reducing Agent (Bio-Rad) and equal volumes loaded onto a 4-12% SDS-PAGE gel (Bio-Rad) for separation followed by transfer to PVDF (Bio-Rad). Membranes were probed with the following antibodies: IκBα (Cell Signaling Technology Cat# 9242, RRID:AB_331623), Cyclophilin B (Cell Signaling Technologies Cat# 43603, RRID:AB_2799247), Runx1 (Abcam Cat# ab92336, RRID:AB_2049267), β-Actin (Santa Cruz Biotechnology Cat# sc-47778 HRP, RRID:AB_2714189).

PCR

Genomic DNA was isolated using a DNeasy Blood and Tissue Kit (Qiagen). Standard PCR to detect the wildtype, floxed, and deleted products for *Runx1* was performed using the following primer set: CCCACTGTGTGCATTCCAGATTGG (Forward), GACGGTGATGGTCAGAGTGAAGC (Reverse 1), CACCATAGCTTCTGGGTGCAG (Reverse 2). Products were run out on a 2% agarose gel alongside a 100 bp ladder (NEB).

Statistical analysis

Unless otherwise indicated, all statistical analyses other than bulk and scRNA-seq were performed using Prism for Mac v6.0h (GraphPad). scRNA-Seq data analyses were performed using an R-based analysis pipeline described below.

Bulk RNA-sequencing

One million FACS-purified neutrophils were isolated as described and stimulated with vehicle or 100 ng/mL LPS for 2 hours prior to RNA isolation. RNA was isolated using TRIzol (Invitrogen) followed by clean up with the low input RNeasy Micro Kit (Qiagen). Three replicates were performed for each condition and genotype (supplemental Figure 6B). To normalize data to total cell number, equal

quantities of the External RNA Controls Consortium Spike-In Control Mix (Ambion) were added to total purified RNA following the manufacturer's instructions. Ultra low input RNA-sequencing library preparation (Genewiz) was followed by paired-end 2 x 150 bp sequencing on an Illumina HiSeq 4000 sequencer. Raw sequencing reads were mapped to the reference mouse genome (mm9) using STAR (v2.6.0a) with default parameter setting (supplemental Table 2).[3] Read counts for each gene were summarized using featureCounts.[4] Normalization with ERCC spike-in control was performed using the R package RUVSeq.[5] Differential expression analysis was performed using edgeR.[6] P-values for differential expression were corrected for multiple-testing using the method of Benjamini-Hochberg. [7]

TLR gene sets were derived from the Kyoto Encyclopedia of Genes and Genomes (KEGG) Pathway database. We included genes from the set "Toll-like receptor signaling pathway" with genes not directly downstream of a TLR removed.[8-10]

scRNA-seq data processing and filtering

Raw sequencing reads were first pre-processed with 10x Genomics Cell Ranger pipeline and aligned to the mouse mm10 reference genome. An initial filtering was performed on the raw gene-barcode matrix output by the Cell Ranger *cellranger count* function, removing barcodes that have less than 1000 transcripts (quantified by unique molecular identifier (UMI)) and 1000 expressed genes ("expressed" means that there is at least 1 transcript from the gene in the cell). Barcodes that pass this filter were considered as cells and were fed into downstream dimension reduction and clustering analysis.

UMAP projection and cell type assignment

To confidently assign cell types, we projected our scRNA-seq data onto a UMAP constructed with BM LK cells from Giladi *et al.* [11] First, we performed PCA on log-transformed expression matrix from Giladi *et al.* using shared variably expressed genes with our data, then used the top 20 PCs to compute a UMAP using the *umap* function from uwot R package ("cosine" distance metric, 10 nearest neighbors,

and default for the rest of the parameters). Using the PCA loading matrix, we projected our data onto the same PCA space as the Giladi *et al*. data, then predicted UMAP embedding using *umap_transform* function with previously computed UMAP model. The final co-embedding of our data with those of Giladi *et al*. is shown in Figure 7.

We noticed that cell-type annotations from Giladi *et al*.[11] do not distinguish neutrophils and neutrophil progenitors at a very fine level. We therefore re-annotated those clusters based on expression of a set of known markers (Figure 7A, left panel). Cells from this study were then annotated with a 3-nearest-neighbor classifier built on the umap co-embedding (Figure 7A, right panel).

Pathway activity analysis

We used AUCell package[12] to compute a per-cell activity score for each pathway in the Reactome database.[13] We slightly modified the standard AUCell pipeline by first ranking genes by Gini coefficient, calculated with fraction-of-expressed-cells across cell types, and retaining those with high Gini (top 25 percentile). The “Area Under the Curve” (AUC) scores were then computed with these variably expressed genes and were used to represent the pathway activity within each cell.

To derive pathways that are differentially active between Runx1 KO and Control LKS^{-} cells along the neutrophil development trajectory, we performed pairwise Student *t* test on the activity score between Runx1 KO neutrophil HPs (CD34+/CD16+, Gstm1+/CD63^{+}, and Fcnb^{+}) and corresponding Control cells (q-value ≤ 0.01). Redundant pathways were removed if the Jaccard index (*number of shared genes/number of all genes)* for the pair of pathways was greater than 0.1 and the pathway had a higher q-value.

SUPPLEMENTAL TABLES

Table S1. Flow cytometry antibodies

Antibody	Fluorophore	Clone	Company	Cat #	RRID
CD3	Biotin	145-2C11	eBioscience	13-0031-85	AB_466320
CD19	Biotin	eBio1D3	eBioscience	13-0193-82	AB_657656
B220	Biotin	RA3-6B2	BioLegend	103204	AB_312989
NK1.1	Biotin	PK136	eBioscience	13-5941-82	AB_466804
Ly6C	BV711	HK1.4	BioLegend	128037	AB_2562630
F4/80	FITC	BM8	eBioscience	11-4801-81	AB_2735037
CD11b	PerCP-Cy5.5	M1/70	BD Pharmingen	550993	AB_394002
Siglec F	PE	E50-2440	BD Pharmingen	552126	AB_394341
Ly6G	PE-Cy7	1A8	BioLegend	127618	AB_1877261
TNF-a	PacBlue	MP6-XT22	BioLegend	506318	AB_893639
F4/80	APC	BM8	eBioscience	17-4801-80	AB_2784647
Streptavidin	BV605	---	BioLegend	405229	---
c-Kit	FITC	2B8	BioLegend	105806	AB_313215
Sca1	PE	D7	BioLegend	108107	AB_313344
B220	APC	RA3-6B2	BioLegend	103212	AB_312997
CD3	APC	145-2C11	BioLegend	100312	AB_312677
CD19	APC	eBio1D3	eBioscience	17-0193-82	AB_1659676
NK1.1	APC	PK136	BioLegend	108710	AB_313397
Gr1	APC	RB6-8C5	BioLegend	108412	AB_313377
CD11b	APC	M1/70	BioLegend	101212	AB_312795
Ter119	APC	TER-119	BioLegend	116211	AB_313712

Comprehensive list of all flow cytometry antibodies used and their corresponding Research Resource Identifier (RRID).

Table S2. RNA-seq mapping summary

Sample	# Read pairs	% Unique mapped
CL1	27,060,148	76.64
CL2	30,469,400	79.41
CL3	31,452,175	77.17
CV1	32,313,026	74.09
CV2	35,027,224	82.57
CV3	31,163,092	74.14
RL1	28,706,853	77.08
RL2	41,591,442	66.01
RL3	36,686,313	76.55
RV1	29,957,508	79.49
RV2	31,797,662	78.04
RV3	32,748,511	79.18

Summary of read mapping from RNA-sequencing analysis of LPS-treated Control neutrophils (CL1, CL2, CL3), vehicle-treated Control neutrophils (CV1, CV2, CV3), LPS-treated Runx1 KO neutrophils (RL1, RL2, RL3), and vehicle-treated Runx1 KO neutrophils (RV1, RV2, RV3).

SUPPLEMENTAL FIGURES

Figure S1. Secretion of cytokines, chemokines, and growth factors by Control and Runx1 KO bone marrow

(A-L) Absolute quantification by CBA of inflammatory factor levels in the supernatant from whole BM cells stimulated for 8 hours with vehicle or 100 ng/mL LPS. Bar graphs depict independent data points. Error bars represent mean ± SD. 5 replicates from 4 experiments were performed for each condition, with all results above the limit of detection (blue arrowhead) plotted. A two-tailed unpaired *t*-test was performed comparing the factor concentration between the Control and Runx1 KO LPS-treated samples (not significant).

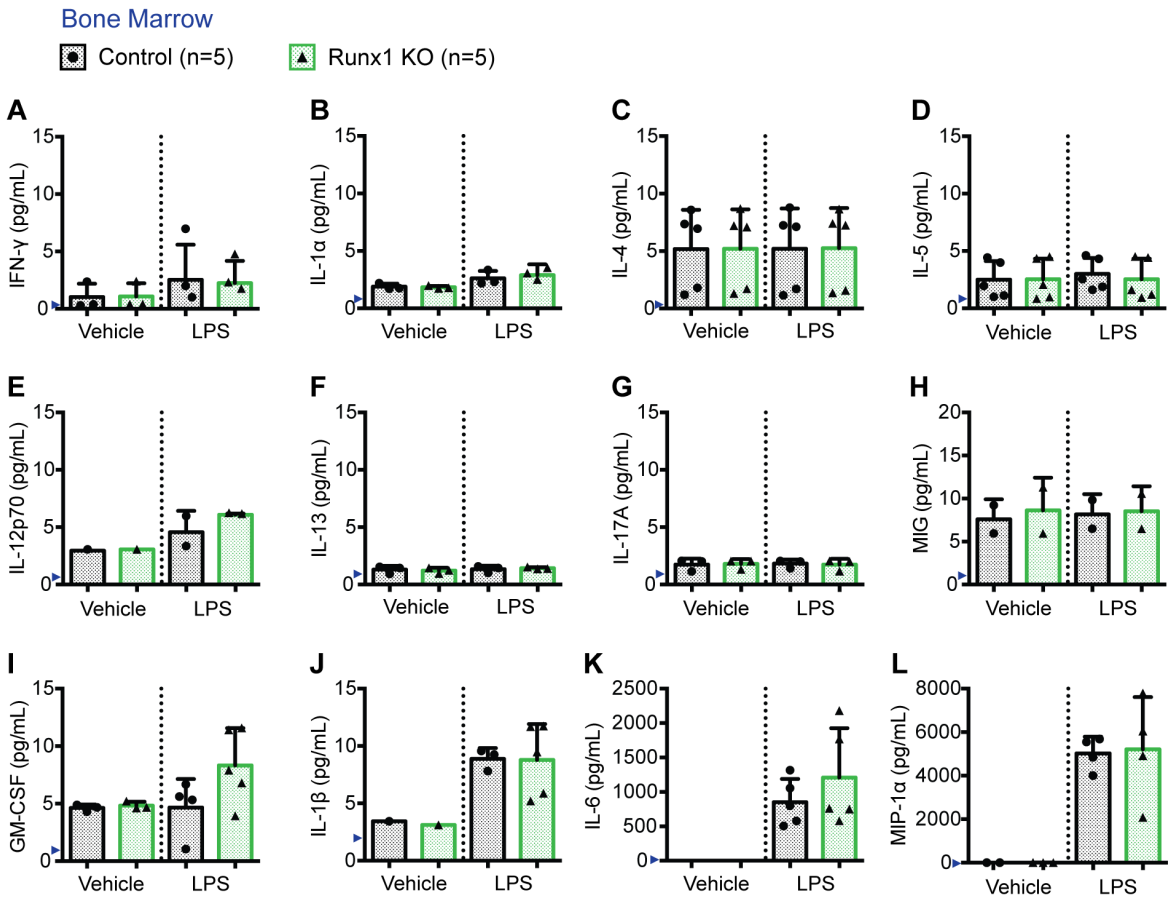

Figure S1. Secretion of cytokines, chemokines, and growth factors by Control and Runx1 KO bone marrow

Figure S2. Gating strategy for myeloid panels

(A) Representative gating strategy of BM monocytes, neutrophils, and eosinophils used to evaluate the phenotypic myeloid compartment. Cells were gated on singlets and dead cells excluded using Zombie Violet. Myeloid cells were gated as Lineage$^-$ (CD3, CD19, NK1.1, B220) and CD11b$^+$. Subsequently, monocytes were gated as Ly6G$^-$ SiglecF$^-$, neutrophils as Ly6G$^+$ SiglecF$^-$, and eosinophils as Ly6G$^-$ SiglecF$^+$. Due to the significantly increased expression of Siglec F on Runx1 KO monocytes (see supplemental Figure 3B) we moved the eosinophil gate higher for Runx1 KO BM so that it would encompass only the well-separated Siglec F^{high}Ly6G$^-$ eosinophil population. (B) Representative gating strategy of BM monocytes and neutrophils utilized for TNF-α intracellular flow assays. Cells were gated on singlets and dead cells excluded using Live Dead Aqua. Monocytes were gated as CD11b$^+$ Ly6G$^-$ and neutrophils as CD11b$^+$ Ly6G$^+$. (C) Representative gating strategy used to sort BM neutrophils and monocytes. Cells were gated on singlets and dead cells excluded using DAPI. Cells were subsequently gated as CD11b$^+$ and Siglec F$^-$. Monocytes were gated as Ly6G$^-$ and neutrophils as Ly6G$^+$ F4/80$^-$. (D) Representative gating strategy used to sort BM Lineage$^-$c-Kit$^+$Sca1$^-$ (LKS$^-$) hematopoietic progenitor cells. Cells were gated on singlets and dead cells excluded using DAPI. Cells were gated as Lineage$^-$ and c-Kit$^+$ and subsequently as c-Kit$^+$ and Sca1$^-$.

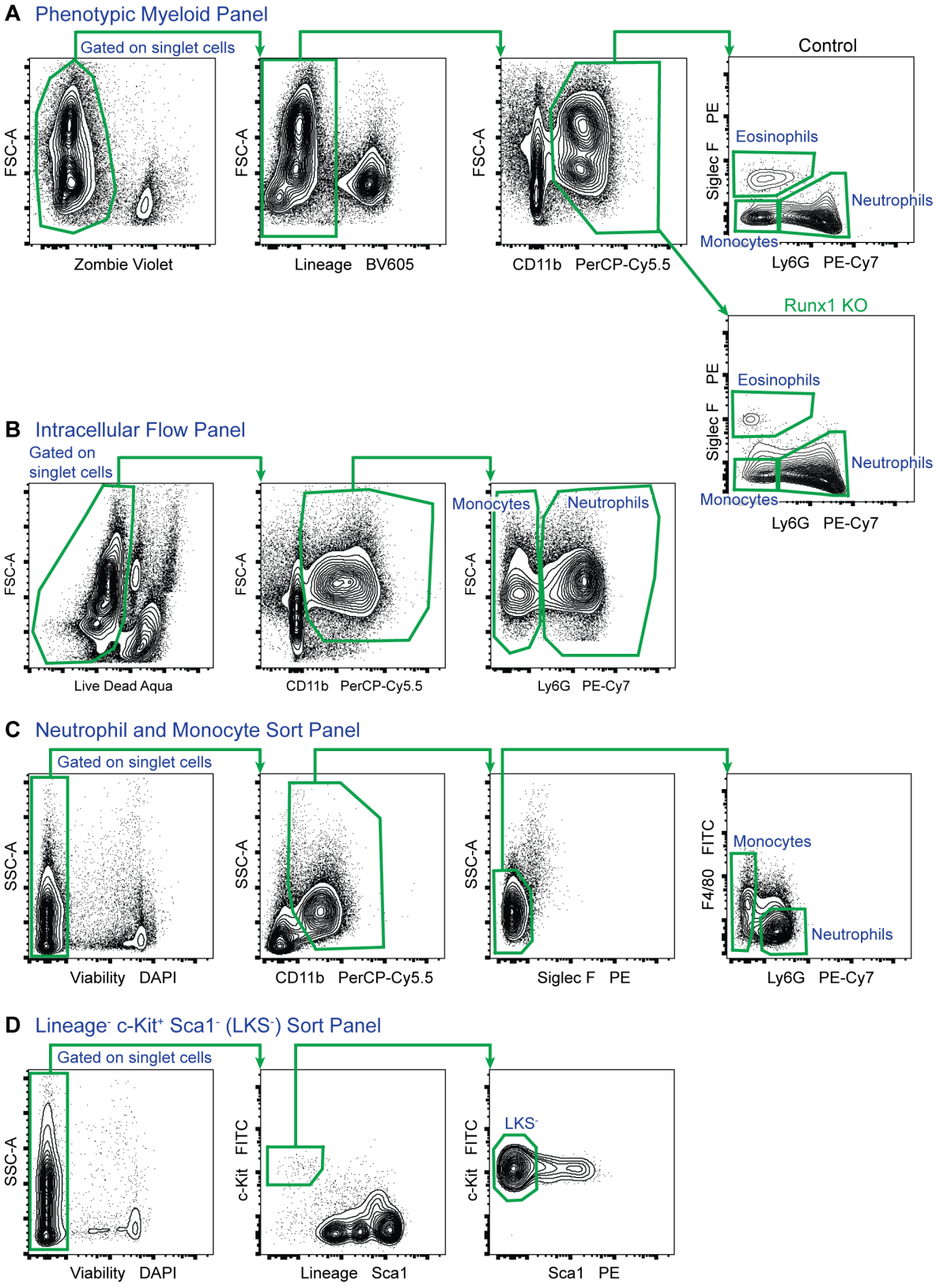

Figure S2. Gating strategy for myeloid panels

Figure S3. Expression of myeloid markers is altered in Runx1 KO bone marrow

(A) Representative histograms showing the expression of Ly6C on Control and Runx1 KO BM neutrophils ($CD11b^+Ly6G^+SiglecF^-$), monocytes ($CD11b^+Ly6G^-SiglecF^-$), and eosinophils ($CD11b^+Ly6G^-SiglecF^+$). Bar graphs depict the frequencies of Ly6C-positive neutrophils, monocytes, and eosinophils (n=3 from 3 experiments, mean ± SD, two-tailed unpaired *t*-test). (B) Representative histograms showing the expression of Siglec F on Control and Runx1 KO BM eosinophils ($CD11b^+Ly6G^-SiglecF^+$). Bar graphs depict relative Siglec F MFI of eosinophils normalized to Control eosinophils run in the same experiment (n=3 from 3 experiments, mean ± SD, two-tailed unpaired *t*-test). *P ≤ 0.05; **P ≤ 0.01; ***P ≤ 0.001

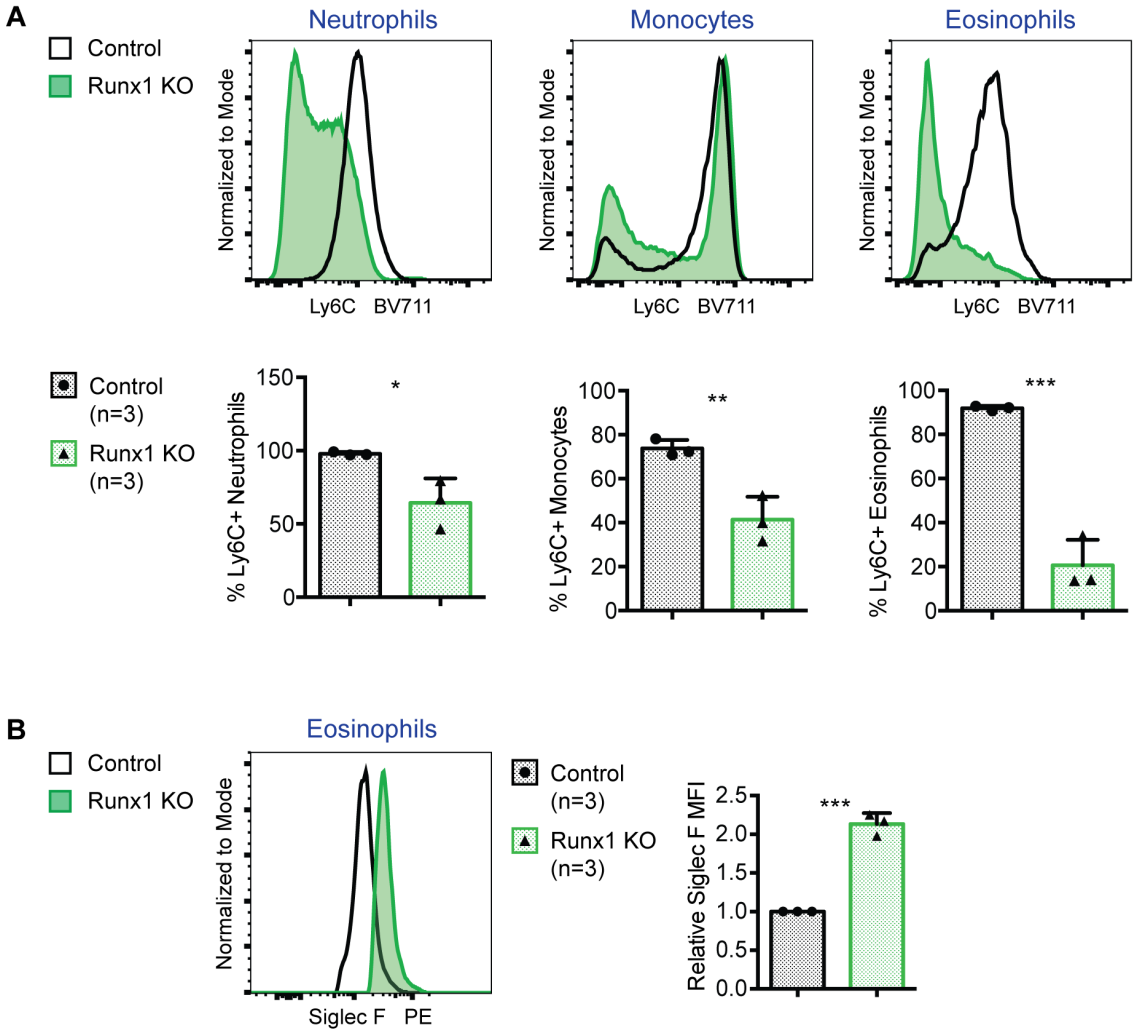

Figure S3. Expression of myeloid markers is altered in Runx1 KO bone marrow

Figure S4. Cytokine production by Runx1 KO monocytes

(A) Quantification of the frequency of TNF-α$^+$ monocytes (CD11b$^+$Ly6G$^-$) after stimulation of whole BM for 4 hours with TLR agonists (n=4-6 from 6 experiments, as indicated). Bar graphs include independent data points with the mean ± SD. A one-way ANOVA followed by Sidak's multiple comparison test to compare the means of the Control and Runx1 KO samples for each TLR agonist was performed (not significant). (B-E) Absolute quantification by CBA of inflammatory factor levels in the supernatant of 200,000 FACS-purified monocytes (CD11b$^+$SiglecF$^-$Ly6G$^-$) stimulated for 8 hours with vehicle or 100 ng/mL LPS. Bar graphs depict independent data points with the mean ± SD. 5 replicates were performed for each condition with all results above the limit of detection (blue arrowhead) plotted. Statistics represent two-tailed unpaired *t*-tests. *P ≤ 0.05; ***P ≤ 0.001; ****P ≤ 0.0001

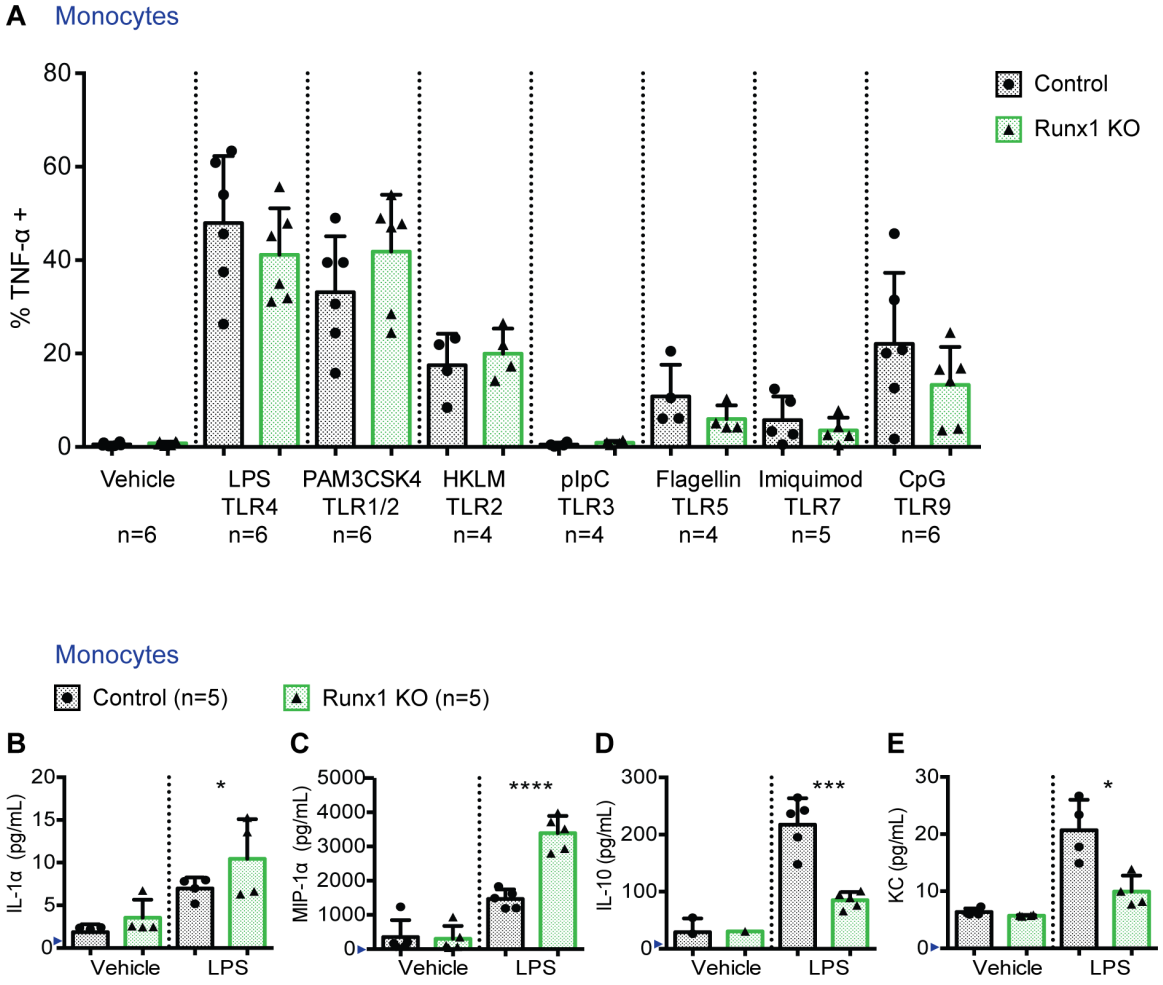

Figure S4. Cytokine production by Runx1 KO monocytes

Figure S5. LPS inhalation supporting materials

(A) Gross appearance of BAL fluid for experiment depicted in Figure 3A-C. In this experiment, there was minimal contamination of the BAL fluid with blood. (B) Second Runx1 KO replicate (Figure 3D) of lung histology showing degree of inflammatory infiltrate, alveolar hemorrhage, and gross damage. This was the only Runx1 KO mouse (1/5) for the experiment depicted in Figure 3D-S that did not demonstrate profound alveolar hemorrhage indicated by either BAL appearance or lung histology. Scale bars, 50 μm.

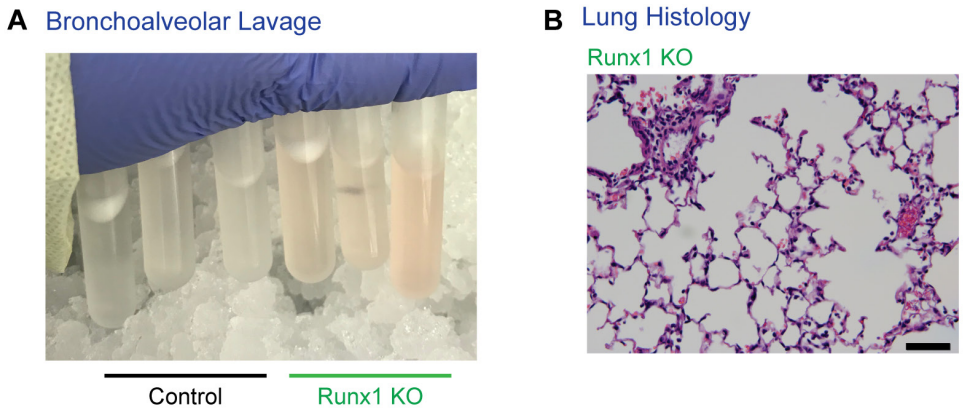

Figure S5. LPS inhalation supporting materials

Figure S6. Neutrophil RNA-seq supporting data

(A) Gene Ontology (GO) analysis of differentially expressed genes down-regulated in vehicle-treated Runx1 KO neutrophils as compared to Controls and up- or down-regulated in LPS-treated Runx1 KO neutrophils as compared to Controls. (B) Pearson correlation of RNA-seq FPKM values across three replicates from 3 independent experiments of LPS-treated Control neutrophils (CL1, CL2, CL3), vehicle-treated Control neutrophils (CV1, CV2, CV3), LPS-treated Runx1 KO neutrophils (RL1, RL2, RL3), and vehicle-treated Runx1 KO neutrophils (RV1, RV2, RV3).

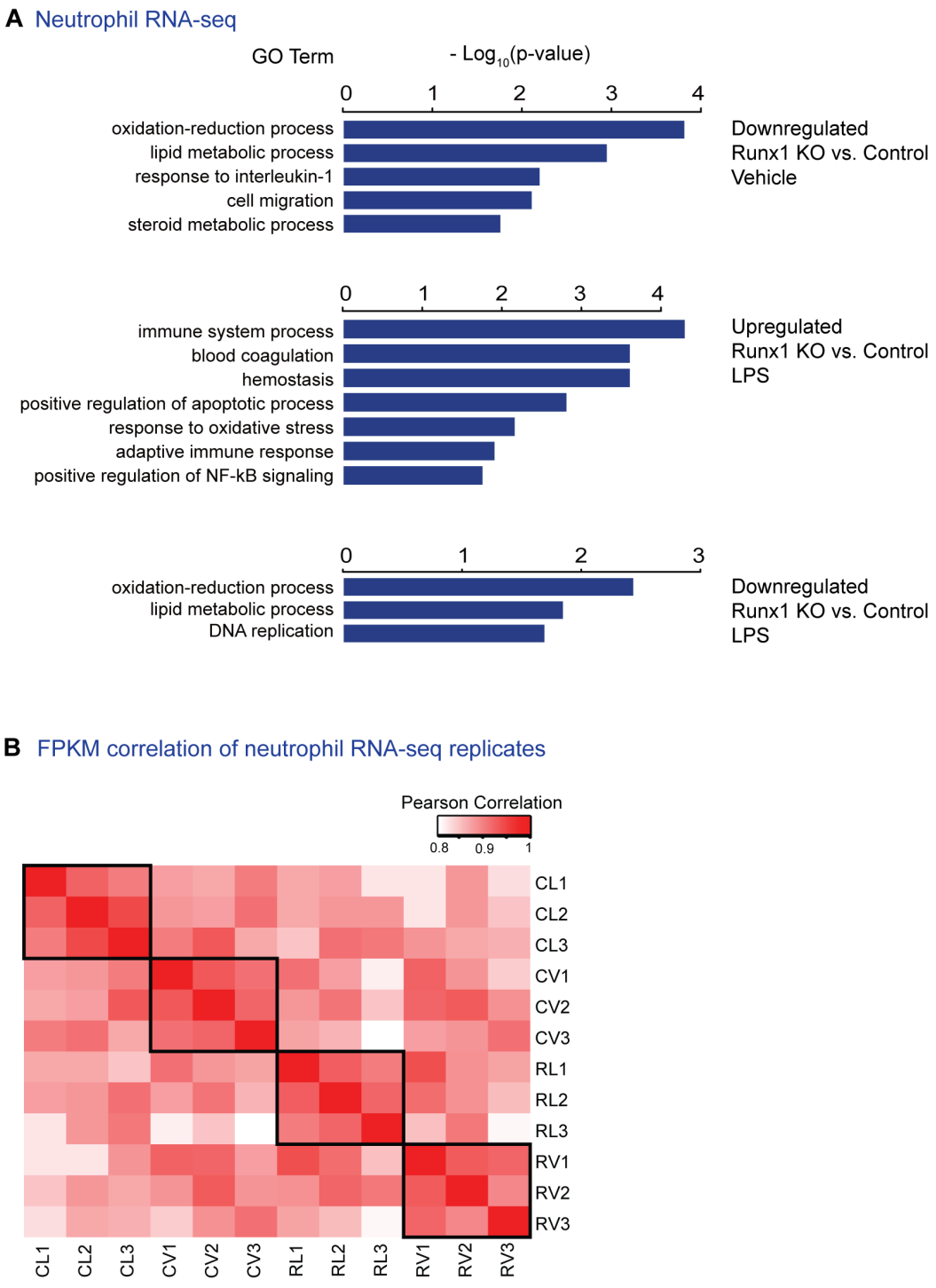

Figure S6. Neutrophil RNA-seq supporting data

SUPPLEMENTAL REFERENCES

1. Jeyaseelan S, Chu HW, Young SK, Worthen GS. Transcriptional profiling of lipopolysaccharide-induced acute lung injury. *Infect Immun*. 2004;72(12):7247-7256.
2. Mei J, Liu Y, Dai N, et al. CXCL5 regulates chemokine scavenging and pulmonary host defense to bacterial infection. *Immunity*. 2010;33(1):106-117.
3. Dobin A, Davis CA, Schlesinger F, et al. STAR: ultrafast universal RNA-seq aligner. *Bioinformatics*. 2013;29(1):15-21.
4. Liou RS, Boone LR, Kiggans JO, et al. Molecular cloning and analysis of the endogenous retrovirus chemically induced from RFM/Un mouse cell cultures. *J Virol* 1983;46:288-292.
5. Risso D, Ngai J, Speed TP, Dudoit S. Normalization of RNA-seq data using factor analysis of control genes or samples. *Nat Biotechnol*. 2014;32(9):896-902.
6. Robinson MD, McCarthy DJ, Smyth GK. edgeR: a Bioconductor package for differential expression analysis of digital gene expression data. *Bioinformatics*. 2010;26(1):139-140.
7. Benjamini Y, Hochberg Y. Controlling the False Discovery Rate - a Practical and Powerful Approach to Multiple Testing. *Journal of the Royal Statistical Society*. 1995;57(1):289-300.
8. Akira S, Takeda K. Toll-like receptor signalling. *Nat Rev Immunol*. 2004;4(7):499-511.
9. O'Neill LA, Golenbock D, Bowie AG. The history of Toll-like receptors - redefining innate immunity. *Nat Rev Immunol*. 2013;13(6):453-460.
10. Kawai T, Akira S. TLR signaling. *Cell Death Differ*. 2006;13(5):816-825.
11. Giladi A, Paul F, Herzog Y, et al. Single-cell characterization of haematopoietic progenitors and their trajectories in homeostasis and perturbed haematopoiesis. *Nat Cell Biol*. 2018;20(7):836-846.
12. Aibar S, Gonzalez-Blas CB, Moerman T, et al. SCENIC: single-cell regulatory network inference and clustering. *Nat Methods*. 2017;14(11):1083-1086.
13. Fabregat A, Sidiropoulos K, Garapati P, et al. The Reactome pathway Knowledgebase. *Nucleic Acids Res*. 2016;44(D1):D481-487.